International Conference on Applied Energy 2019
Aug 12-15, 2019, Västerås, Sweden
Paper ID: 0118

INVESTIGATION OF WIND FARM INTERACTION WITH ETHIOPIAN ELECTRIC POWER'S GRID: A CASE STUDY AT ASHEGODA WIND FARM

Fikremariam Beyene[1], Getachew Bekele [2*]

Addis Ababa University

ABSTRACT

Ethiopia is currently moving forward with various projects to raise the power generation capacity in the country. The progress observed in the recent years indicates this fact clearly and indisputably. The rural electrification program, the modernization of the power transmission system, and the development of wind farms are some worth mentioning. It is well known, wind power is globally embraced as one of the most important sources of energy mainly for its environmentally friendly characteristics, and also that once it is installed it is a source available free of charge. However, integration of wind power plant with an existing network has many challenges that need to be given serious attention. In Ethiopia a number of wind farms are either installed or under construction with a series of them are in plan to be erected in the near future. Ashegoda Wind farm (13°2'N, 39°6'E), which is the subject of this study, is the first large scale wind farm under construction with the capacity of 120 MW. The first phase of the 120 MW, which is 30 MW has been completed and is expected to be connected to the grid soon. This paper is concerned with the investigation of the wind farm interaction with national grid under transient operating condition. The main concern is the fault ride-through (FRT) capability of the system when the grid voltage drops to exceedingly low values because of short circuit fault and also the active and reactive power behavior of wind turbines after the fault is cleared. On the wind turbine side, a detailed dynamic modelling of variable speed wind turbine of a 1 MW capacity running with a squirrel cage induction generator and full-scale power electronics converters is done and analyzed using simulation software DIgSILENT PowerFactory. On the Ethiopian Electric Power Corporation side, after having collected sufficient data for the analysis, the grid network is modeled. In the model, FRT capability of the plant is studied by applying 3-phase short circuit on the grid terminal near the wind farm. The results show that the wind farm can ride from voltage deep within short time and the active and reactive power performance of the wind farm is also promising.

Keywords: Squirrel cage induction generator, active and reactive power, DIgSILENTPowerFactory, fault ride-through capability, 3-phase short circuit.

NONMENCLATURE

Abbreviations	
DSL	Dynamic Simulation Language
FRT	Fault ride-through Capability
MPPT	Maximum Power Point Tracking
PWM	Pulse Width Modulation
RF	Rotor Flux Control
Symbols	
n	Year

1. INTRODUCTION

Over the last 20 or so years, renewable energy sources have been attracting great attention due to the cost increase, limited reserves, and adverse environmental impact of fossil fuels. In the meantime, technological advancements, cost reduction, and governmental incentives have made some renewable energy sources more competitive in the market. Among them, wind energy is one of the fastest growing renewable energy sources [1].

In Ethiopia in terms of generation capacity; studies

Selection and peer-review under responsibility of the scientific committee of the 11th Int. Conf. on Applied Energy (ICAE2019).

estimate the total national potential for grid based wind electricity system to be about much more than 10 GW [2]. This shows that there is a favorable condition to construct large scale wind farm.

The wind power generations influence the stability of the power system, so that it must meet the standardization like FRT requirement which is necessary during the wind farm is fault condition.

Due to the fact that wind generators are much smaller in capacity than conventional power generators, high number of turbines need to be used. That implicates the use of model aggregation techniques for dynamic simulation, within reasonable calculation time. Hence, aggregated wind park, represented by equivalent wind generator, is considered in this paper.

2. WIND CONOVERSION SYSTEM

Wind turbines' mechanical components comprise of the blades and rotor, rotor shaft, gearbox, generator shaft and generator as shown in Fig. 1. The turbine rotor shaft speed and torque are determined by the wind speed and blade pitch. The gearbox provides a speed adjustment to the generator's shaft. The electrical system comprises of the induction generator, Generator Side Converter, DC link and Grid Side Converter

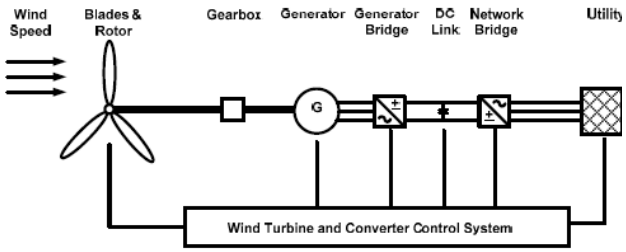

Fig 1 Variable speed wind turbine with squirrel-cage induction generator (full-scale power electronics) [3]

2.1. Wind turbine model

Equation (1) shows the aerodynamic equation of a wind turbine that relates mechanical power to wind speed and mechanical speed of the turbine [4].

$$P_t = \frac{\rho}{2}\pi R^2 u_w^3 C_P(\lambda,\theta) \quad (1)$$

P_t : Mechanical power of the wind turbine, ρ : Air density, R: Rotor radius, λ: Tip speed ratio, θ: Blade pitch angle, C_P: Power coefficient of function of λ and θ, u_w: Wind speed.

The tip speed ratio λ: is defined as follows.

$$\lambda = \frac{\omega_t R_r}{u_w} \quad (2)$$

With ω_t being the mechanical frequency of the wind turbine.

Equation (1) defines the steady state aerodynamic behavior of wind turbine; it cannot reflect dynamic stall effect correctly. An approximate method for including dynamic stall effect is described in [5].

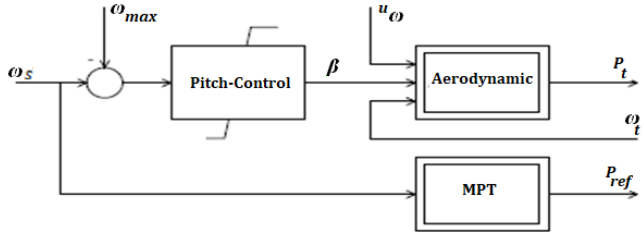

Fig 2 Generic wind Turbine effect

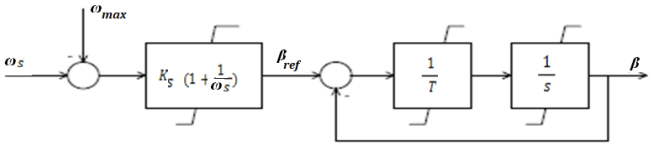

Fig 3 Generic model of the pitch control system

A generic wind turbine model for stability studies based on a maximum power point tracking strategy [9] can be implemented according to figure 2.

In case rotor frequency below$\boldsymbol{\omega_{max}}$, it is the maximum power tracking (mpt) characteristics that defines the active power regulation, which depends on the shaft speed. The power reference is that of the set value of the power controller. Once the shaft speed reaches its maximum, then the set point for the active power remains constant and the pitch angle controller (figure 3) acts to drive the shaft speed back to maximum permissible limit

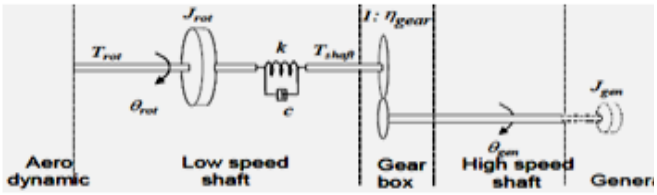

Fig 4 Drive train models [7]

Drive train is considered since it has the most significant influence on the power fluctuations. The other parts of the wind turbine structure, e.g. tower and the flap bending models do not have significant effect on grid interaction of wind farm [6].In most cases two-mass drive train model is used as it provides more accurate drive train dynamic responses and substantially improves simulation efficiency [7]

$$\omega_k = \omega_{rot} - \frac{\omega_{gen}}{n_{gear}} \quad (3)$$

$$\dot{\omega}_{rot} = \frac{\tau_{rot} - \tau_{shaft}}{J_{rot}} \quad (4)$$

$$\tau_{shaft} = c\omega_k + k\theta_k \quad (5)$$

Where: ω_{gen} and ω_{rot} are generator and rotor angular speeds respectively; θ_{k} and ω_{k} are the angles and angular speed differences between the two ends of the flexible shaft respectively; $\mathrm{J_{rot}}$ is rotor inertia; τ_{rot} and τ_{shaft} are aerodynamic torques on low and high speed shafts respectively; k and c are the low speed shaft stiffness and a damping coefficient respectively; $\mathrm{n_{gear}}$ is gear ratio which is 1:67 in this work as the wind turbines are gearless. Similar to aerodynamic model, Drive train model is implemented by DSL future of DIgSILENTPowerFactory.

2.2. *Squirrel Cage Induction Generator Model*

It is known that the two-phase synchronous reference frame where the q-axis is 90° ahead of the d-axis in the direction of rotation can be used to derive the dynamic model of SCIG.However,the electrical model of SCIG in the synchronous reference frame is given by (6) and (7), where the quantities on the rotor side have been referred to the stator side. The model is composed of two groups, i.e. the first is the voltage equations and the other is the flux ones [6]. ***ω, β***

$$\begin{cases} v_{ds} = R_s i_{ds} + \frac{di_{ds}}{dt} - \omega_s \lambda_{qs} \\ v_{qs} = R_s i_{qs} + \frac{di_{qs}}{dt} + \omega_s \lambda_{ds} \\ v_{dr} = 0 = R_r i_{rs} + \frac{d\lambda_{dr}}{dt} - (\omega_s - \omega_r)\lambda_{qr} \\ v_{qr} = 0 = R_r i_{qr} + \frac{d\lambda_{qr}}{dt} + (\omega_s - \omega_r)\lambda_{dr} \end{cases} \quad (6)$$

$$\begin{cases} \lambda_{ds} = L_s i_{ds} + L_m i_{dr} \\ \lambda_{qs} = L_s i_{qs} + L_m i_{qr} \\ \lambda_{dr} = L_r i_{dr} + L_m i_{ds} \\ \lambda_{qr} = L_r i_{qr} + L_m i_{qs} \end{cases} \quad (7)$$

where subscripts 's' and 'r' refer to the stator and rotor sides respectively, subscripts 'd' and 'q' refer to the d-axis and q axis respectively. *Lm* is the mutual inductance.

The electromagnetic torque can be calculated as

$$T_e = \lambda_{qs}\, i_{ds} - \lambda_{ds} i_{qs} \quad (8)$$

The active and reactive power transmitted through the stator can be calculated as

$$\begin{cases} P_s = v_{ds} i_{ds} + v_{qs} i_{qs} \\ Q_s = v_{ds} i_{qs} - v_{qs} i_{ds} \end{cases} \quad (9)$$

2.3. *Power converter*

The generator- and grid-side converters are self-commutated converters and are usually set-up by six-pulse bridges according to Figure 5.

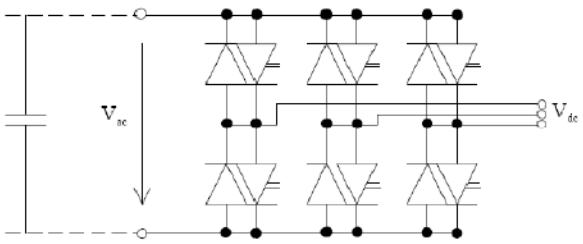

Fig 5 PWM-converter circuits [10]

For a perfect DC-voltage and perfect PWM modulation (infinite modulation frequency), the fundamental frequency, the RMS value of the line to line voltage, and the DC voltage can be given by equation 10.

$$|U_{ac}| = \frac{\sqrt{3}}{2\sqrt{2}} p_m U_{dc} \quad 10$$

The AC-voltage phase angle is defined by the PWM converter.

The pulse-width modulation factor *Pm* is the control variable of the PWM converter. Equation (10) is valid for$0 \le p_m < 1$. For values larger than 1 the converter starts saturating and the level of low order harmonics starts to increase. The converter model is completed by the power conservation equation:

$$U_{dc} I_{DC} + \sqrt{3} R_e (U_{ac} I_{ac}^*) = 0 \quad 11$$

Once again, this equation assumes an ideal converter (loss free). The reason is that the switching frequency of the PWM converter is usually very high, typically several hundred Hz. It is to be noted that earlier on assumption is made that it is a perfect converter. It is obvious that the average switching losses are proportional to $\mathbf{u_{dc}^2}$, where the proportionality constant is the resistance and can be considered to be that between the two dc-poles for the fundamental frequency model.

2.3. Frequency converter controller Model

The control of the frequency converter of the SCIG is done from both sides; one from the grid side and the other from the generator side. Coordination between the frequency converter control and that of the blade angle control of the rotor blades is maintained. The complete model is shown in Figure 6. The models for yellow parts are available as built in models while others are to be developed.

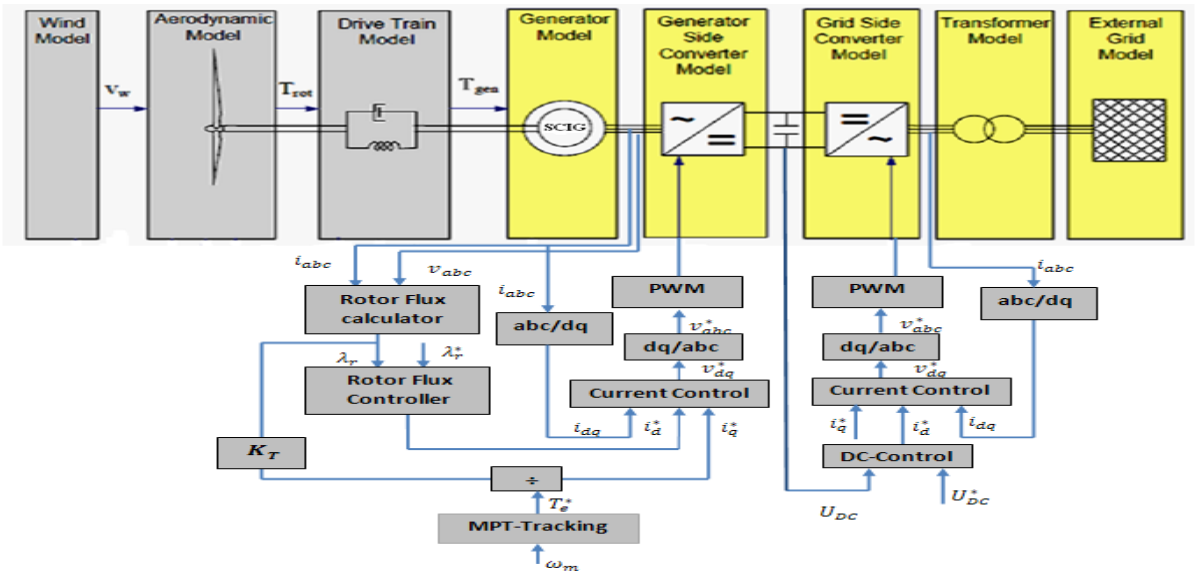

Fig 2 Modeling scheme and control concept of the variable speed WT with SCIG

2.5. *Grid side converter control*

The aim of the control of the grid side converter is to maintain the dc-link capacitor voltage to a set value regardless of the magnitude and direction of the rotor power and to guarantee a converter operation with unity power factor (zero reactive power). This means that the grid side converter exchanges only active power with the grid, and therefore the transmission of reactive power from SCIG to the grid is done only through the stator.

With respect to the reference frame oriented along the grid voltage vector position, the control enables the independent control of active and reactive power exchanges between the grid and the converter (Figure 6). The d-current is utilized to control the DC voltage and q-current to regulate the reactive power [6].

The grid side converter control contains two PI control loops in cascade:

- A very fast (inner) converter current control.
- A slower (outer) DC-voltage control loop

E.i. The Inner current control loop

The current controller loop is a fast-inner current control loop and it is part of the cascaded control strategy. It needs to be faster compared to the outer controllers so that to achieve control system stability.

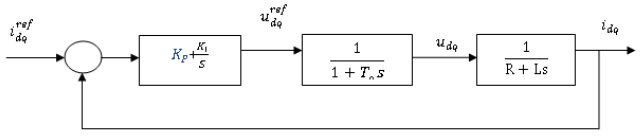

Fig 7 reduced form of the inner current control loop

The tuning of current controller by modulus optimum criteria can be obtained from the open loop transfer function of the current controller figure 8.

$$G_{ol}(s) = K_P\left(\frac{1+sT_i}{sT_i}\right)\left(\frac{1}{1+sT_a}\right)\left(\frac{1}{R+sL}\right) \qquad 12$$

Using Matlab the following step response is obtained with specifications: Rise time $t_r = 0.299 \times 10^{-3}$s , settling time $t_s = 0.838 \times 10^{-3}$s, maximum over shoot $M_P = 4.58\%$ peak time $t_P = 0.615 \times 10^{-3}$s and peak amplitude 1.05.

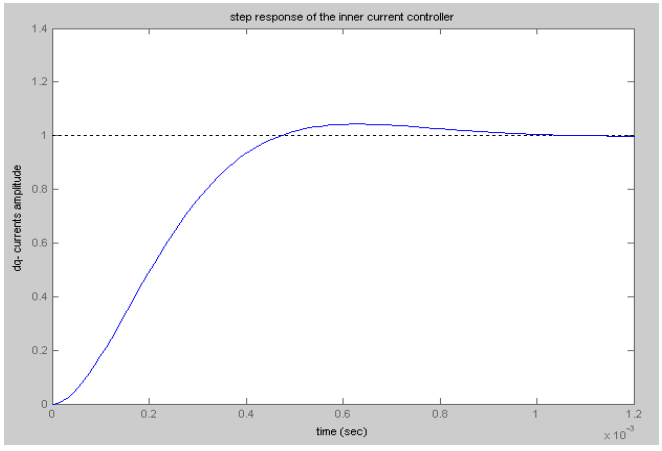

Fig 8 Step response of the inner current control loop

E.ii. DC-voltage control loop

DC voltage control is important for controlling the power exchange between the converters. The DC voltage

control aimed at keeping the DC voltage at a defined value using the converter current as a control variable.

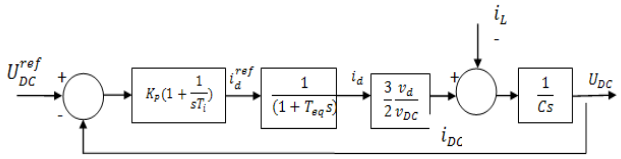

Fig 9 Block diagram representation of the DC voltage control loop

The overall closed loop transfer function from figure 9 becomes:

$$G_{cl} = \frac{KT_i s + K}{T_i T_{eq} C s^3 + T_i C s^2 + KT_i s + K} \qquad 13$$

where, $K = \frac{3}{2}\frac{K_P v_d}{V_{DC}}$

The following step response is obtained using Matlab with Rise time 0.000675 s, peaking time 0.00181 s, peak amplitude 1.25, and settling time 0 .00473 s is achieved.

a. Control of generator-side Converter

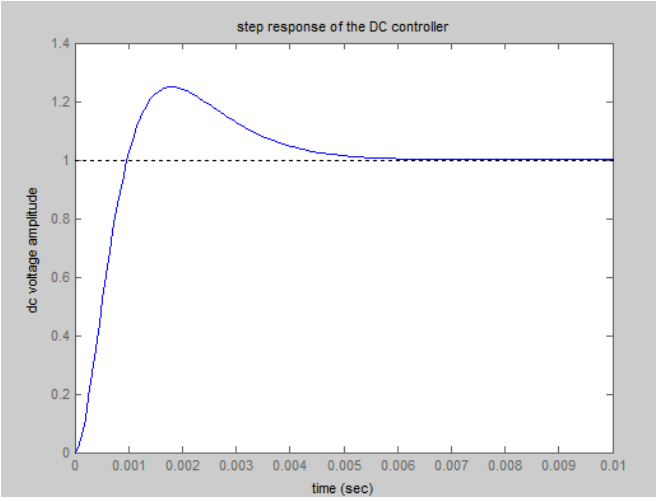

Fig 10 Step response of the designed DC voltage control loop

2.6. *Control of Generator-Side Converter*

In variable-speed squirrel cage induction generator (SCIG) wind energy conversion systems (WECS), full-capacity power converters are required to adjust the speed of the generator in order to harvest the maximum possible power available from the wind. The generator-side converter (rectifier) is used to control the speed or torque of the generator with a maximum power point tracking (MPPT) scheme.

The generator side converter control consists of two PI- control loops in cascade

- Rotor flux control loop
- A very fast (inner) stator current control loop.

2.6.1 Tuning Rotor flux Controller

Rotor flux controller loop controls flux of the rotor.

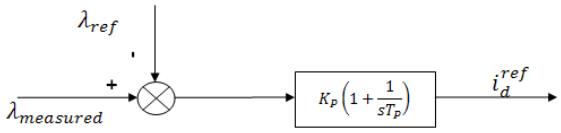

Fig 11 The RF-controller

2.6.2 *Tuning the current controller*

Tuning of generator side current controller is the same as procedure followed on the grid side current controller. The tuning of current controller by modulus optimum criteria can be obtained from the open loop transfer function of the current controller figure 7.

$$G_{ol}(s) = K_P\left(\frac{1+sT_i}{sT_i}\right)\left(\frac{1}{1+sT_a}\right)\left(\frac{1}{R+sL}\right) \qquad 14$$

Using Matlab the following step response is obtained with specifications: Rise time $t_r = 0.299 \times 10^{-3}s$, settling time $t_s = 0.838 \times 10^{-3}s$, maximum over shoot $M_P = 4.57\%$ peak time $t_P = 0.615 \times 10^{-3}s$ and peak amplitude 1.05.

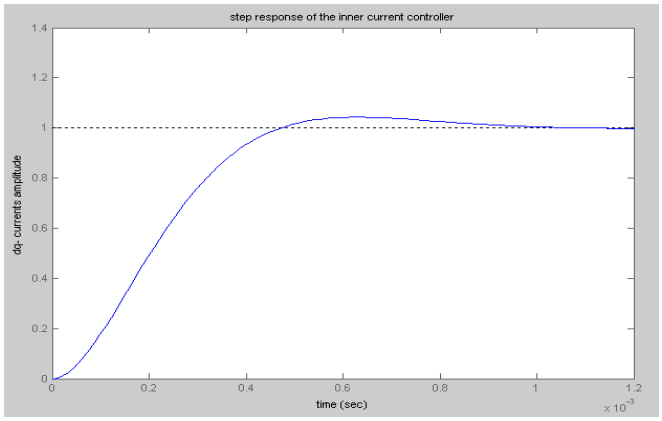

Fig 1 Step response of the inner current control loop with the designed current controller

2.7. W*ind farm Layout*

The dynamic performance of wind farm with grid connected full-scale squirrel cage induction generator with gearbox is analyzed on the basis of a typical wind farm layout of phase-I with a total rated power of 30 MW and a nominal frequency of 50 Hz.

The wind farm is connected to EEPCo's 230 kV Mekele Substation via 20km of overhead line. The electrical network is the 230 kV bus in the Mekele substation has

been modeled as voltage source (slack bus).The 30 wind generators have a rated voltage of 0.69 kV. Each wind turbine is connected by underground AC cables to a step-up transformer to 33 kV. These transformers are then connected at 230 kV to one 63MVA, 230 kV/33 kV step-up transformer. The wind farm configuration is shown in Figure 13.

the integration of the wind farm to the grid. According to the grid connection conditions from E.ON [8] for squirrel cage induction generator machines, is applied to the PCC and the generator response in this study.

As shown, in Figure 15, simulation results of a 3-phase fault with 150 ms duration at constant wind conditions. The figures show the voltage at the PCC as

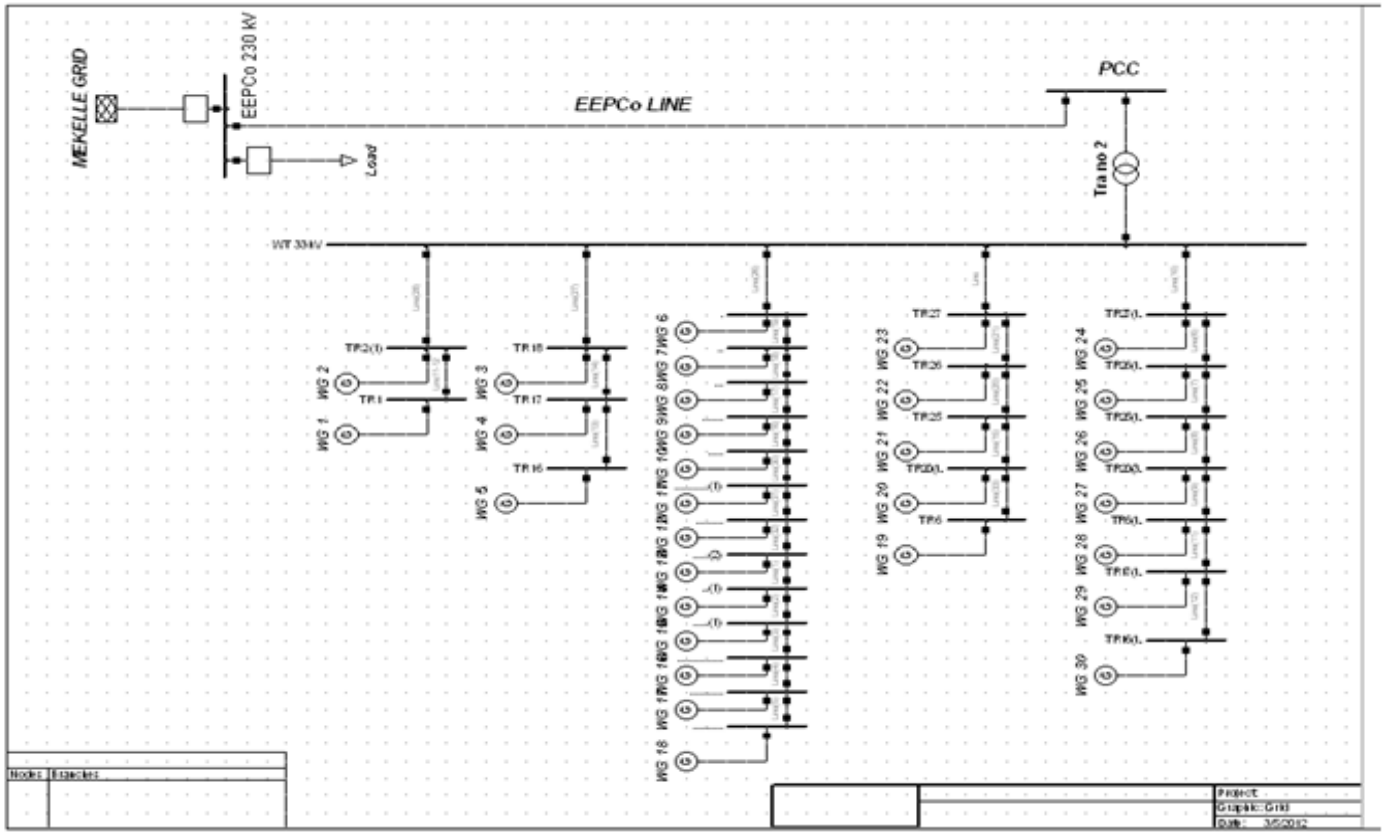

Fig **13** Typical wind farm layouts with 30 wind turbines of Ashegoda Wind Farm

2.8. Simulation and Analysis

It is known that Ethiopia has embarked on using large scale wind form. However, there is no any standard for

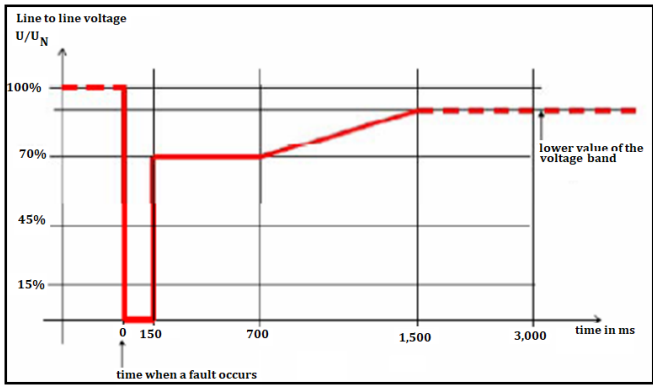

Fig 14 Voltage profile according to the requirements for LVRT capability of synchronous generators according to [8]

well as the voltage atthe generator terminals, generator rotor speed, total active power and total reactive power for supply to grid.

It shows that before the application of three phase short circuit faults (pre-fault value) at wind turbine terminal the terminal voltage was almost 1.0 p. u. Then after the application of three phase short circuit faults the terminal generator terminal voltage dipped to 0.49 p. u which almost falls to 49%. After application of fault clearance the terminal voltage restored to pre-fault value after 1.52 s.

Considering the capability of the active and reactive power at the wind turbine terminals it returns to the pre fault value after the fault is cleared. As shown in Figure 17, the active power just before the occurrence of the three-phase short circuit fault was 30MW. When the fault occurs the active power falls to 0.034MW and then,

when the fault is cleared then the active power returns to almost its pre fault value within time duration of 1402ms.

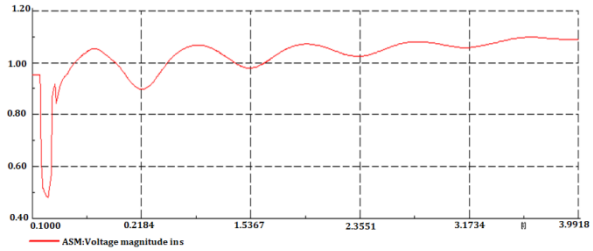

Fig **15.** Voltage at generator terminal

The reactive power just before the occurrence of the fault was -20.495Mvar as shown in Figure 18. Clearance of the fault would result in the change of the value of the reactive power to support the voltage to return to its pre-fault value there by the reactive power itself returns to its pre-fault value after 1122ms.

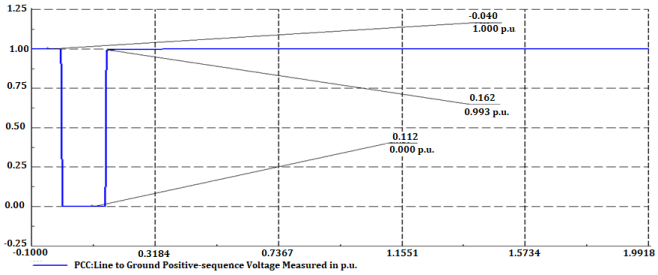

Fig **16**Voltages at Points of Common Coupling (PCC)

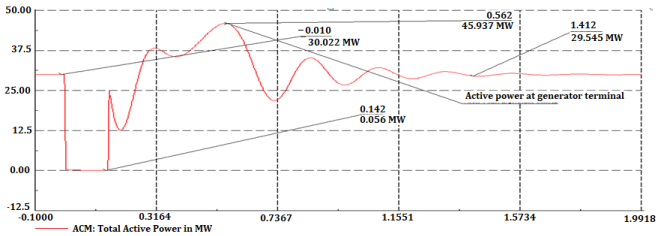

Fig **17**Active power at generator terminal

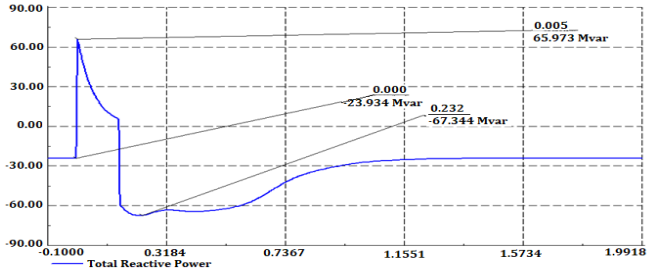

Fig **18** Reactive Power at generator terminal

3. CONCLUSION

In this paper dynamic behavior of variable speed wind turbine with squirrel cage connected to EEP grid is analyzed. The response of the wind turbine for short circuit condition exhibits good performances. Comparison of the simulation results with previous requirements [8] shows that Ashegoda wind farm can ride from voltage deep within a short period of time and can be said is with a measurably good performance of the active and reactive power for a wind farm. This clearly shows its immunity to 3-phase short-circuit fault according to the designed control system.

The parameters of 1 MW wind turbine of this paper are described in Table 1 and parameters of power system and equipment in Table 2 to Table 5.

Table 1 Parameters of wind turbine model

Generator	Asynchronous
Rated power(MW)	1
Rated Voltage(kV)	0.69
Rotor diameter (m)	61
Rated Wind speed(m/s)	15
Rated rotor speed(rpm)	12-23
Gear Ratio:	1:67

Table 2 Parameters of Transformers

Transformer	Rated power(MVA)	Rated Voltage (KV)	% impedance
Transformer No. 1	1.25	33/0.69	12
Transformer No. 2	63	230/33	12

Table 3 Parameters of Network

Network	Rated (KV)	S"k	
		S"k Max	S"k Min
Mekele	230	967.6454	808.1743

Table 4 parameters of line

Rated Voltage (kV)	Positive sequence (ohm/km)		Zero sequence (ohm/km)		Susceptance (Microsecond/km)	
	R1	X1	R0	Xo	C0	C1
230	0.092	0.3139	0.0918	1.1513	0.0069	0.0114

Table 5 Parameters of PI control

	RF Control	DC Control	Gen-side Inner current Control	Grid-side Inner current Control
K_P	5	306.76	1.76	3.29
T_i	0.01	0.0018	0.144	0.269

REFERENCE

[1] H. Polinder, F. F. A. Van der Pijl, G.-J. de Vilder, and P. J. Tavner, "Comparison of Direct-Drive and Geared Generator Concepts for Wind Turbines", IEEE Transactions on Energy Conversion, Vol. 21, No. 3, 725-733, 2006.

[2] Solomon YismawAgaje, "Techno-economic and financial evaluation of wind energy in Ethiopia Ashegoda Wind Farm Project 120 MW as case study", Msc. Thesis, KTH School of Industrial Engineering and Management Department of Energy Technology, 2011.

[3] Markus A. P¨oller "Doubly-Fed Induction Machine Models for Stability Assessment of Wind Farms", Power Tech Conference Proceedings, 2003 IEEE Bologna, 2004

[4] Sørensen, PoulEjnar; Hansen, Anca Daniela; Janosi, L.; Bech, J.; Bak-Jensen, B. "Simulation of Interaction between Wind Farm and Power System",Technical-Report, Risoe-R-128(EN),ISBN 87-550-2912-4, ISBN 87-550-2913-2 (Internet) ISSN 0106-2840

[5]Tao Sun, Z Chen, FredeBlaabjerg, "Transient analysis of gridconnected wind turbines with DFIG after an external short-circuit fault," in 2004 Nordic Wind Power Conference, pp.1-5

[6] M. Benchagra, M. Ouassaid "Study and Analysis on the Control of SCIG and its Responses to Grid Voltage Unbalance" Multimedia Computing and Systems (ICMCS), 2011 International Conference, 2010

[7] R.Pena, J.C.Clare, G.M.Asher, "Doubly fed induction generator using back-to-back PWM converters and its application to variable speed wind-energy generation," IEE Proc. Electric Power Applications, vol.143, no.3, pp.231-241, May 1996.

[8] E.OnNetz GmbH, "Netzanschlussregeln fur Hoch-und Hochstspannung, April 2006"

t Inc,2Electric Machines Identification and Control Laboratory, Department of Applied Sciences,University of Quebec at ChicoutimiQuebecCanada.

[10] DIgSILENT GmbH "DIgSILENTPowerFactory V13 - User Manual,"DIgSILENT GmbH, 2002